

PAPER • OPEN ACCESS

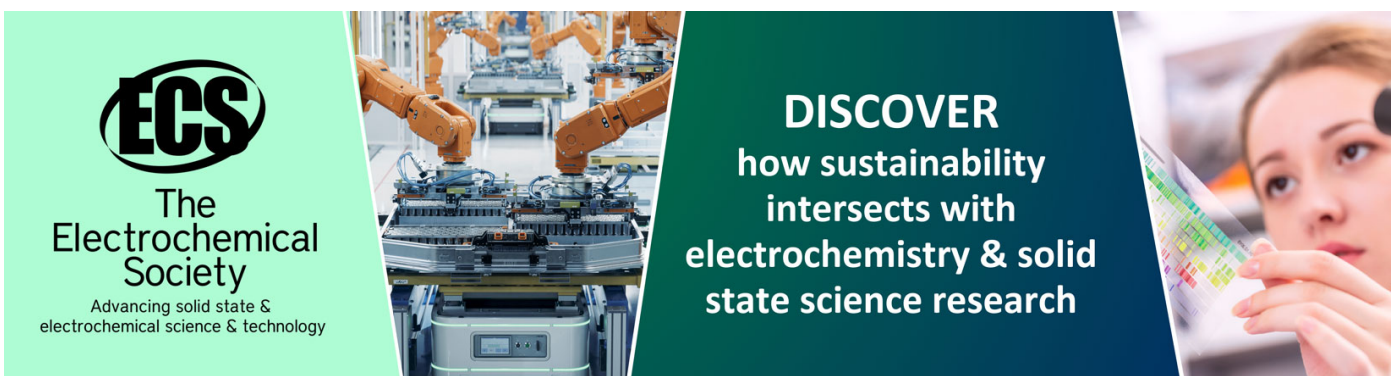
Microstructure features of Ni-based and Ti-based alloys formed by method of wire-feed electron beam additive technology

To cite this article: D A Gurianov *et al* 2019 *IOP Conf. Ser.: Mater. Sci. Eng.* **597** 012042

View the [article online](#) for updates and enhancements.

You may also like

- [Numerical analysis on the effect of process parameters on deposition geometry in wire arc additive manufacturing](#)
Shilong FAN, , Fei YANG et al.
- [Investigation on the performance of wire electrical discharge machining \(WEDM\) using aluminium matrix composites \(AMCs\) micro-channel](#)
Mahamood Ansari and Imtiaz Ali Khan
- [Determination of enthalpy, temperature, surface tension and geometry of the material transfer in PGMAW for the system argon-iron](#)
E Siewert, J Schein and G Forster



ECS
The
Electrochemical
Society
Advancing solid state &
electrochemical science & technology

DISCOVER
how sustainability
intersects with
electrochemistry & solid
state science research

Microstructure features of Ni-based and Ti-based alloys formed by method of wire-feed electron beam additive technology

D A Gurianov, K N Kalashnikov, V Utyaganova, E S Khoroshko and A V Chumaevskii

Institute of Strength Physics and Materials Science of the Siberian Branch of the Russian Academy of Sciences, pr. Akademicheskii, 2/4, Tomsk, 634021, Russia

Corresponding author: desa-93@mail.ru

Abstract. In the present study, a microstructural investigation of wire-feed EBAM-manufactured nickel-based and titanium-based alloys were conducted by producing single wall sample with 16 and 19 vertical layers, respectively. It was shown that in obtained material microstructural and elemental gradient presents. The results of the research show that dendrites and grains grow epitaxial in the direction of temperature gradient. Non-directional dissipation of heat on the edge of the sample leads to formation of equiaxed structure. Chosen parameters allow to produce low-defective samples by EBAM technology.

1. Introduction

Additive manufacturing is a group of processes used to obtain products from their three-dimensional models. These processes implement a layer-by-layer deposition and until forming a nearly net shape product. Additive technologies are classified [1] by type of the feed material (powder or wire) and heat source (laser, electron beam, arc). Metals, polymers, ceramics and composites can be used as source materials. The additive manufacturing is characterized by the local layer-by-layer deposition of the material until forming a compact product. The homogeneity of melting and solidification of the material is the most important aspect for obtaining qualitative and durable products. The layer-by-layer growing is a complicate system of heat and mass transfer processes. As a rule, such a complicate process may result in appearance of defects such as hot cracks, interlayer separation, pore formation due to incomplete melting and deformation in cooling. Deformation is caused by difference in temperature expansion coefficients between wire and substrate materials [2, 8]. The final microstructure determines the mechanical properties of the product and in its turn depends on the technological parameters of the product formation such as energy density, growing speed and wire-feed rate. Selection of optimal parameter values is necessary for obtaining products with mechanical properties comparable or superior to those of products obtained by traditional methods of casting and metalworking. Due to the fact that the microstructure of the material determines its mechanical properties, control and optimization of the microstructure is an important and urgent task [3, 5, 14].

In accordance with the terminology adopted in American Society for Testing and Materials the wire-feed electron-beam additive manufacturing of metallic components, relates to a class known as Directed Energy Deposition (DED-technologies). The DED-systems are characterized by a high productivity, effective energy input, supplying raw materials directly to the molten pool, possibility of applying



material to existing parts/substrates and low cost consumables [6]. DED-technologies allow obtaining large nearly net shape components, which require minor mechanical treatment. The DED technologies are most widely used in the aerospace, defense, and petrochemical industries.

The wire-feed additive manufacturing allows making products during layer-by-layer process of metal wire deposition. The deposition is carried out sequentially using some suitable deposition strategy to form a three-dimensional shape. This technology can be used to obtain products from a wide range of materials, including titanium alloys, nickel and copper-nickel alloys, aluminum alloys, alloyed steels, tungsten, etc. [8]. Titanium-based alloys are also used both in aircraft and in biomedical industries. Whereas the nickel-based superalloys are used for production of complex and critical parts of the hot section in a modern gas-turbine engine-building industry for aviation and energy. Nowadays expensive nickel-based superalloys with directional solidification are used for production blades of gas-turbine engines. These superalloys contain up to 10wt.% of rare-earth metals such as rhenium, ruthenium, cerium, yttrium, lanthanum. However, the introduction of rhenium contributes to the selection of undesirable topologically close-packed phases that adversely affect the properties of the material. The modern technology of casting products with directional solidification is also expensive and the yield of products does not exceed 80%. It occurs due to the fact that new crystallization seed can form on the walls of injection molds, due to the high growth rate. Additive manufacturing doesn't have such problem. In case of damage to the product from such superalloy, it is more profitable to apply repairing rather than replace the entire part [15]. Most modern papers [3, 4, 13] dedicated to the organization of directional solidification in the additive process use powdered feed material and a laser as a heat source. This approach is characterized by specific defects - residual pores [4], to eliminate which it is necessary to carry out hot isostatic pressing, which increases the cost of production. The use of electron-beam additive manufacturing makes it possible to organize directional solidification in a formed product and the use of the considered economically doped nickel superalloy allows reducing production costs. Despite the advantages, such a combination of material and technology is completely not considered in modern literature. In addition, the structure of the product obtained by this method is close to the cast state, which is important for nickel-based superalloys and titanium-based alloys.

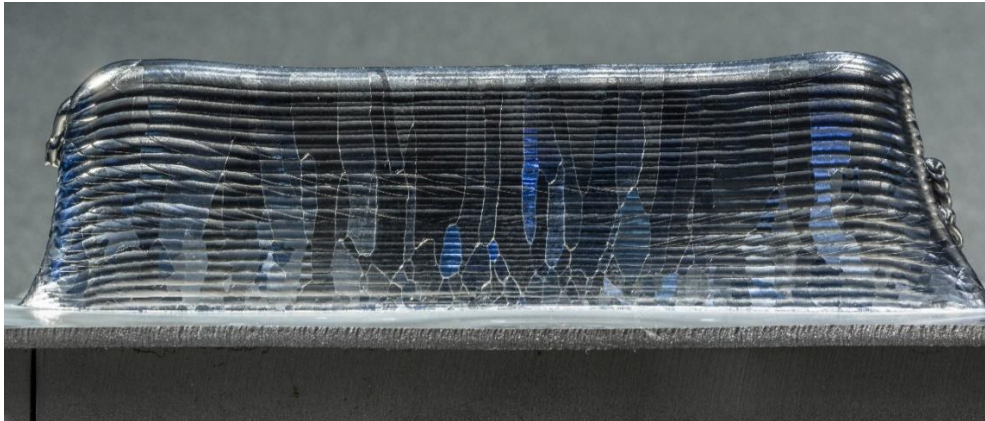
The purpose of this study is to identify the characteristics of the formation of the macro and microstructure of the material of metal products obtained using wire-feed electron beam additive manufacturing.

2. Material and methods

Nickel-based superalloy ZhS6U (brand chemical composition presented in table 1) and titanium-based alloy Ti-6Al-4V wire filaments were used as raw materials. Formation of vertical walls was carried out in a vacuum chamber with chosen parameters of accelerating voltage (25-35 kV), electron beam current (30-50 mA) and beam scan frequency (1000 Hz). Products obtained on the installation were described in the previous work [7]. A Ti-6Al-4V alloy wall consisted of 20 layers and had a height 23 mm (Fig. 1). A wall made of ZhS6U alloy consisted of 16 layers and had a height of 19 mm. Transverse and longitudinal polished and etched metallographic cross-sections were prepared for investigation of macro- and microstructure of material of walls. Cross-sections of products from an alloy of ZhS6U were etched in the Marble's reagent ($\text{CuSO}_4 - 8 \text{ g}$, $\text{HCl} - 40 \text{ ml}$, $\text{H}_2\text{O} - 40 \text{ ml}$) within 10 seconds [9]. Cross-sections of products from an alloy of Ti-6Al-4V were etched in Kroll's reagent ($\text{HF} - 2 \text{ ml}$, $\text{HNO}_3 - 6 \text{ ml}$, $\text{H}_2\text{O} - 92 \text{ ml}$) within 15 seconds [10]. Metallographic investigations were carried out using Olympus LEXT OLS 4100 laser confocal scanning microscope. Microstructure was studied on scanning electron microscope LEO EVO 50.

Table 1. Chemical composition (% wt.) of alloy ZhS6U [11]

W	Ni	Al	Co	Cr	Mo	Nb	Ti
9.5-11.0	54.3-62.7	5.1-6	9-10.5	8-9.5	1.2-2.4	0.8-1.2	2-2.9

**Figure 1.** General view of the product from titanium alloy Ti-6Al – 4V in the form of a vertical wall.

3. Results and discussion

The macrostructure of the material of the titanium alloy wall in longitudinal section is presented in Figure 2. As can be seen, the epitaxial growth of columnar grains occurs along almost the full wall's height. The concentration of quasi-equiaxial grains increases as approaching to the edges of the sample. This phenomenon can be explained by the fact that three dimensional heat dissipation occurs at the boundary of each of the deposited layers. It is caused by heat removal into the vacuum chamber space in the form of radiation, as well as through the previously formed layers of the product into the substrate and a cooled worktable. The radiation component of cooling makes a significantly less contribution into heat removal for metal volumes of material far from the surface. In this case, the prevailing direction of heat removal flux is directed along the temperature gradient to the substrate and the cooled worktable that is why the columnar grains are formed.

It is known [4] that there is a dependence of the grain morphology and the microstructure on the ratio temperature gradient (G)/solidification rate (R) (Figure 3). Thus, as the value of G decreases and the value of R increases, the morphology of the elements of the microstructure changes in the following order: planar, cellular, cellular dendrites, columnar dendrites, equiaxial (for titanium-based alloys: columnar, mixed, equiaxed grains). On this basis, it can be assumed that in the newly applied layers the ratio $G/R < 1$, which leads to the formation of grains with a morphology close to equiaxial. A similar ratio holds for the edges of the grown wall. Directed grain growth occurs when $G/R > 1$. The columnar grains have an average length of 16.07 ± 4.63 mm and a width of 2.39 ± 0.77 mm. Grains with a morphology close to equiaxed have an average diameter of 0.86 ± 0.29 mm. In addition, pores of up to 0.6 mm in size are present in the investigated sample.

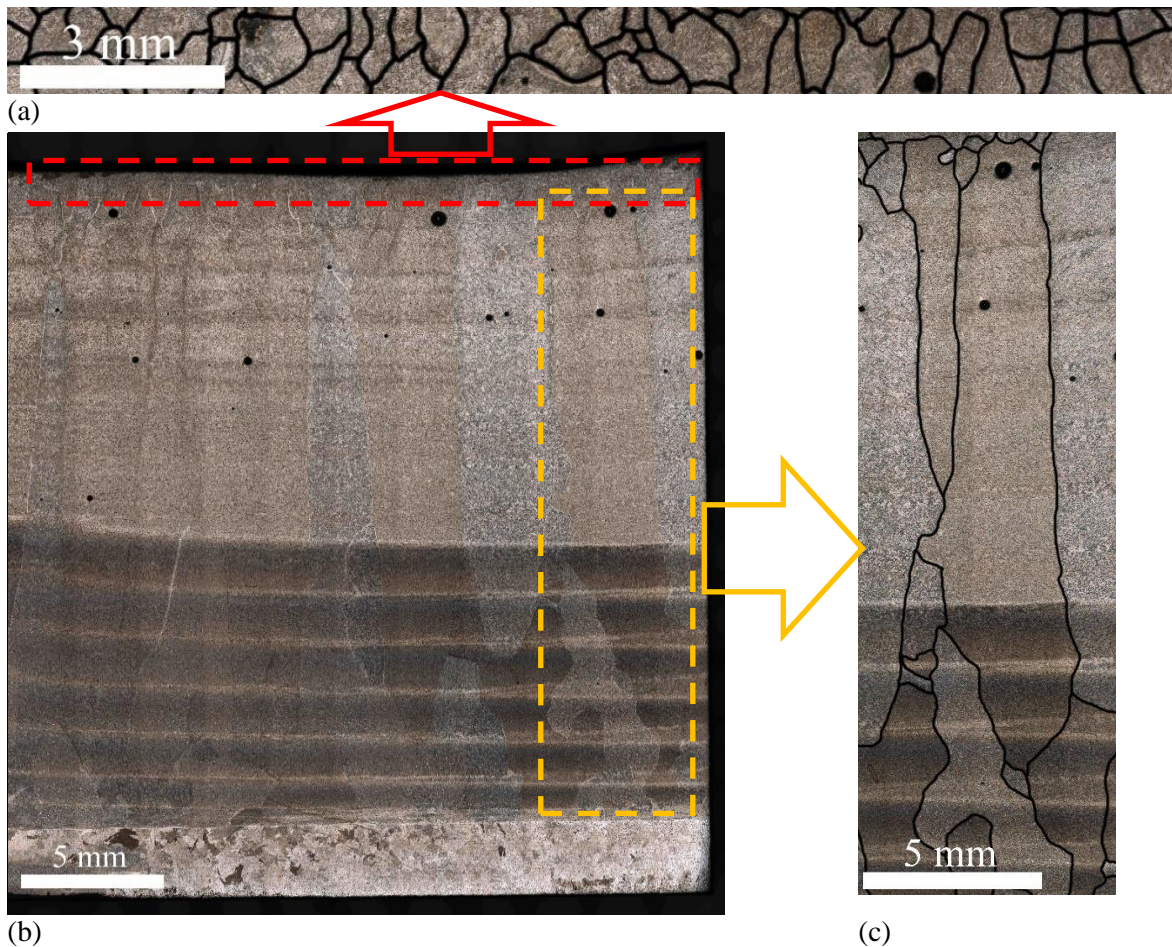


Figure 2. Metallographic images of macrostructure of titanium alloy Ti-6Al-4V wall obtained by wire-feed electron-beam additive technology. (a) – equiaxed grains in top of sample, (b) – panoramic images, (c) – columnar grains in bulk of sample.

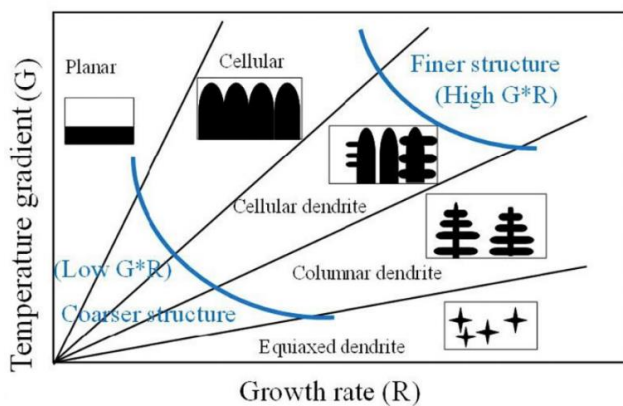


Figure 3. The effect of temperature gradient (G) and growth rate (R) on the solidification morphology and size [4].

Images of the microstructure of the heat-resistant nickel-based alloy ZhS6U are presented in Figure 4. Analysis of the entire cross-sectional area of the wall shows that a thin layer of irregular dendrites is on the border with the substrate, then dendrites form with a morphology close to equiaxial, and then dendrite growth begins mainly in the direction of additive growth (shown in Figure 4 by arrows). Dendrites grow in one direction in groups of 5-30 pieces; the difference in the direction of growth of groups can reach 90°. The morphology of the elements of the structure changes from directed to

equiaxed, as in the case of titanium alloy, as approaching to the edge. The same transition can be observed at the interlayer boundary. The SEM images of the ZhS6U alloy show a skeletal structure formed in the upper part of the product by the primary and secondary dendrites' arm system [12]. As the distance from the substrate increases, the structure changes from coarse to fine. It indicates on the increase in the temperature gradient and crystallization rate, according to [4]. It is known that $(G \times R)$ is related to the primary dendrite arm spacing according to equation as follows:

$$\lambda = a(G \times R)^n \quad (1)$$

where λ (μm) is the primary dendrite arm spacing, a ($^\circ\text{C}$) is the parameter proportional to the solidification interval ΔT , G ($^\circ\text{C} / \text{cm}$) is the temperature gradient, R (m/s) is the solidification ratio, n is the fractional dimensionless number varying from 1/4 to 1/2. Due to these two facts, it can be argued that an increase in the product of $(G \times R)$ values is indeed taking place ($G \times R$).

The microstructure image allows observing gray (dendrite arms) and dark gray (interdendritic spaces) areas. The secondary phase precipitates represented by white particles along the boundaries of arms have a needle shape (in the upper part of the sample) and a complex morphology near the substrate. These phases belong to the γ/γ' -eutectic, carbides (MC, M_6C , M_{23}C_6) and topologically close-packed phases (Laves - Ni_3Nb , σ - CrCo, μ - $\text{Co}_7(\text{Mo}, \text{W})_6$). It is also noticeable that these phases are thinned at the boundaries of the layers and become gray. Elemental analysis suggests a lower Al and Ti and high Co contents in the dendrites whereas increased contents of Ti, W and Nb is detected in the secondary phases.

The presence of pores was not detected on the investigated cross-section views. However, the presence of cracks was established. The most probable mechanism of cracks formation is the blocking of interdendrite spaces with carbides in the solidification process, which leads to the formation of micropores from which cracks develop during the shrinkage [13].

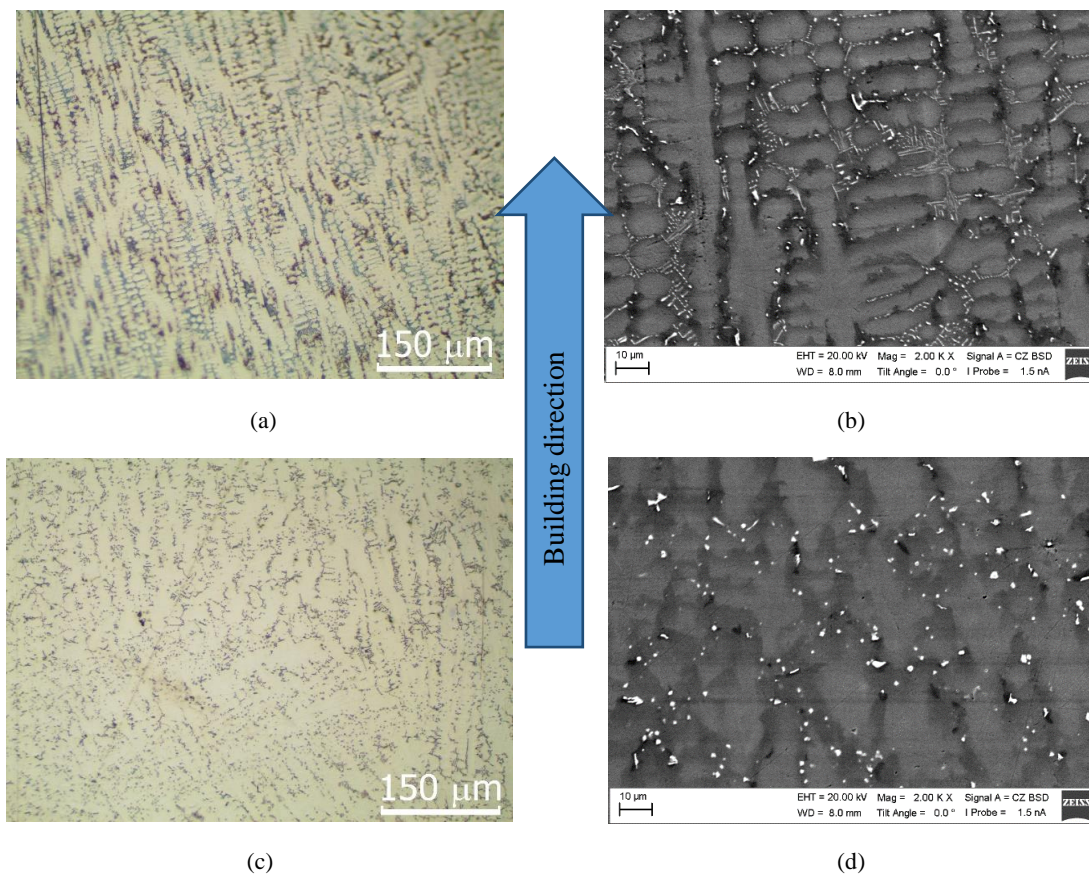


Figure 4. Metallographic (a, c) and SEM (b, d) images of macro- and microstructure in transverse section of vertical wall from alloy ZhS6U. Top area – (a, b), bottom area – (c, d).

4. Conclusions

Both macro- and microstructure of products made of Ti-6Al-4V and ZhS6U alloys using the additive wire-feed electron-beam technology were investigated. The results of the study show that titanium grains and dendrites in a nickel-based superalloy grow epitaxially along the direction of the temperature gradient through the previously formed layers of the product into the substrate and the cooled worktable. In addition, it was shown that directional solidification occurs only in the bulk of the samples. The reason for such an effect is the omnidirectional three-dimensional heat dissipation at the boundary of the sample, including one by radiation cooling. It is established that nickel alloy specimens are less defective than titanium ones.

Acknowledgments

This work was performed within the frame of the Fundamental Research Program of the State Academies of Sciences for 2013-2020, line of research III.23.

References

- [1] Vayre B., Vignat F., Villeneuve F. 2012 *Mechanics and Industry*. **13(2)** 89
- [2] Vastola G., Zhang G., Pei Q.X., Zhang Y.W. 2015 *Additive Manufacturing*. **7** 57
- [3] Sahoo S., Chou K. 2016 *Additive Manufacturing*. **9** 14
- [4] Karimi P., Sadeghi E., Åkerfeldt P., Ålgårdh J., Andersson J. 2018 *Materials and Design* **160** 427
- [5] Tarasov S., Filippov A., Savchenko N., Fortuna S., Rubtsov V., Kolubaev E., Psakhie S. 2018 *International Journal of Advanced Manufacturing Technology*. **99** 2353
- [6] Kalashnikov K.N., Khoroshko E.S., Kalashnikova T.A., Chumaevskii A.V., Filippov A. 2018 *Journal of Physics Conference Series*. **1115** 042049
- [7] Filippov A., Fortuna S.V., Gurianov D.A., Kalashnikov K.N. 2018 *Journal of Physics Conference Series*. **1115** 042044
- [8] Kolubaev A.V., Tarasov S., Filippov A., Denisova Yu.A., Kolubaev E.A., Potekaev A.I. 2018 *Russian Physics Journal*. **61(5)** 1491
- [9] Gontcharov A., Yuan Tian, et. al. 2019 *Journal of Engineering for Gas Turbines and Power*. **141** / 041031-1
- [10] Yuwei Zhai, Haize Galarraga, Diana A. Lados 2016 *Engineering Failure Analysis*. **69** 3
- [11] Kablov E., Petrushin N., Parfenovich P. 2018 *Metal Science and Heat Treatment*. **60** 106
- [12] J. A. Brooks, A. Thompson, and J. Williams 1984 *Weld. J.* **63** 71
- [13] Zhipeng Zhou, Lan Huang, et. al. 2018 *Materials and Design*. **160** 1238
- [14] Nikonov A.Yu., Zharmukhambetova A.M., Ponomareva A.V., Dmitriev A.I. 2018 *Phys. Mesomech.* **21(1)** 43
- [15] Lei Z., Lu N., Yu X. 2019 *Journal of Manufacturing Processes*. **42** 11